Improved tools for the Brainbow toolbox

Dawen Cai[1,2], Kimberly B Cohen[1,2], Tuanlian Luo[1,2], Jeff W Lichtman[1,2] & Joshua R Sanes[1,2]

In the transgenic multicolor labeling strategy called 'Brainbow', Cre-*loxP* recombination is used to create a stochastic choice of expression among fluorescent proteins, resulting in the indelible marking of mouse neurons with multiple distinct colors. This method has been adapted to non-neuronal cells in mice and to neurons in fish and flies, but its full potential has yet to be realized in the mouse brain. Here we present several lines of mice that overcome limitations of the initial lines, and we report an adaptation of the method for use in adeno-associated viral vectors. We also provide technical advice about how best to image Brainbow-expressing tissue.

The discovery that recombinant jellyfish GFP fluoresces when expressed in heterologous cells[1] has led to a vast array of powerful methods for marking and manipulating cells, subcellular compartments and molecules. The discovery or design of numerous spectral variants[2–13] (fluorescent proteins collectively called XFPs; ref. 14) expanded the scope of the 'GFP revolution' by enabling discrimination of nearby cells or processes labeled with contrasting colors. At least for the nervous system, however, two or three colors are far too few because each axon or dendrite approaches hundreds or thousands of other processes in the crowded neuropil of the brain.

Several years ago, we developed a transgenic strategy called Brainbow[15] that addresses this problem by marking neurons with many different colors. In this method, three or four XFPs are incorporated into a transgene, and the Cre-*loxP* recombination system[16] is used to make a stochastic 'choice' of a single XFP to be expressed from the cassette. Because multiple cassettes are integrated at a single genomic site, and the choice within each cassette is made independently, combinatorial expression can endow individual neurons with 1 of ~100 colors, providing nearby neurons with distinct spectral identities.

If Cre recombinase is expressed transiently, descendants of the initially marked cell inherit the color of their progenitor. Accordingly, the Brainbow method has been adapted for use in lineage analysis in non-neural tissues of mice[17–21]. In addition, it has been adapted for analyses of neuronal connectivity, cell migration and lineage in fish[22,23] and flies[24,25]. In contrast, the method has been little used in the mouse nervous system[26]. We believe that the main reasons for this are limitations of the initial set of Brainbow transgenic mice. These include suboptimal fluorescence intensity, failure to fill all axonal and dendritic processes, and disproportionate expression of the 'default' (that is, nonrecombined) XFP in the transgene. We have now addressed several of these limitations, and we present here a new set of Brainbow reagents. In addition, we provide guidelines for imaging Brainbow-expressing tissue.

RESULTS

Design of Brainbow 3.0 transgenes

As a first step in improving Brainbow methods, we sought XFPs with minimal tendency to aggregate *in vivo*, high photostability and maximal stability with respect to paraformaldehyde fixation. Because some XFPs that ranked highly in cultured cells performed poorly *in vivo*, we generated transgenic lines from 15 XFPs (**Supplementary Table 1** and refs. 2–13). Of the XFPs tested in this way, seven were judged suitable: mTFP1, EGFP, EYFP, mOrange2, TagRFPt, tdTomato and mKate2.

From these XFPs, we chose three according to the criteria of minimal spectral overlap and minimal sequence homology. These XFPs were mOrange2 from a coral (excitation peak (Ex) = 549 nm, emission peak (Em) = 565 nm), EGFP from a jellyfish (Ex = 488 nm, Em = 507 nm) and mKate2 from a sea anemone (Ex = 588 nm, Em = 635 nm)[2,9,11]. Our reason for minimizing sequence homology was to ensure that the XFPs would be antigenically distinct, in contrast to spectrally distinct but antigenically indistinguishable jellyfish variants (EBFP, ECFP, EGFP and EYFP). Exploiting this property, we generated antibodies to the XFPs in different host species (rabbit anti-mCherry, anti-mOrange2 and anti-tdTomato; chicken anti-EGFP, anti-EYFP and anti-ECFP; and guinea pig anti-mKate2, anti-TagBFP and anti-TagRFP; **Supplementary Table 1**). Tests in transfected cultured cells confirmed a lack of cross-reactivity (data not shown).

Next we addressed the need to fill all parts of the cell evenly. Unmodified XFPs labeled somata so strongly that nearby processes were difficult to resolve, whereas palmitoylated derivatives, which targeted the XFPs to the plasma membrane, were selectively transported to axons and labeled dendrites poorly[15]. We therefore generated farnesylated derivatives[27], which were trafficked to membranes of all neurites (see below).

On the basis of these results, we generated 'Brainbow 3.0' transgenic lines incorporating farnesylated derivatives of mOrange2, EGFP and mKate2. We retained the Brainbow 1 format[15], in which

[1]Center for Brain Science, Harvard University, Cambridge, Massachusetts, USA. [2]Department of Molecular and Cellular Biology, Harvard University, Cambridge, Massachusetts, USA. Correspondence should be addressed to J.R.S. (sanesj@mcb.harvard.edu).

RECEIVED 3 OCTOBER 2012; ACCEPTED 30 MARCH 2013; PUBLISHED ONLINE 5 MAY 2013; DOI:10.1038/NMETH.2450

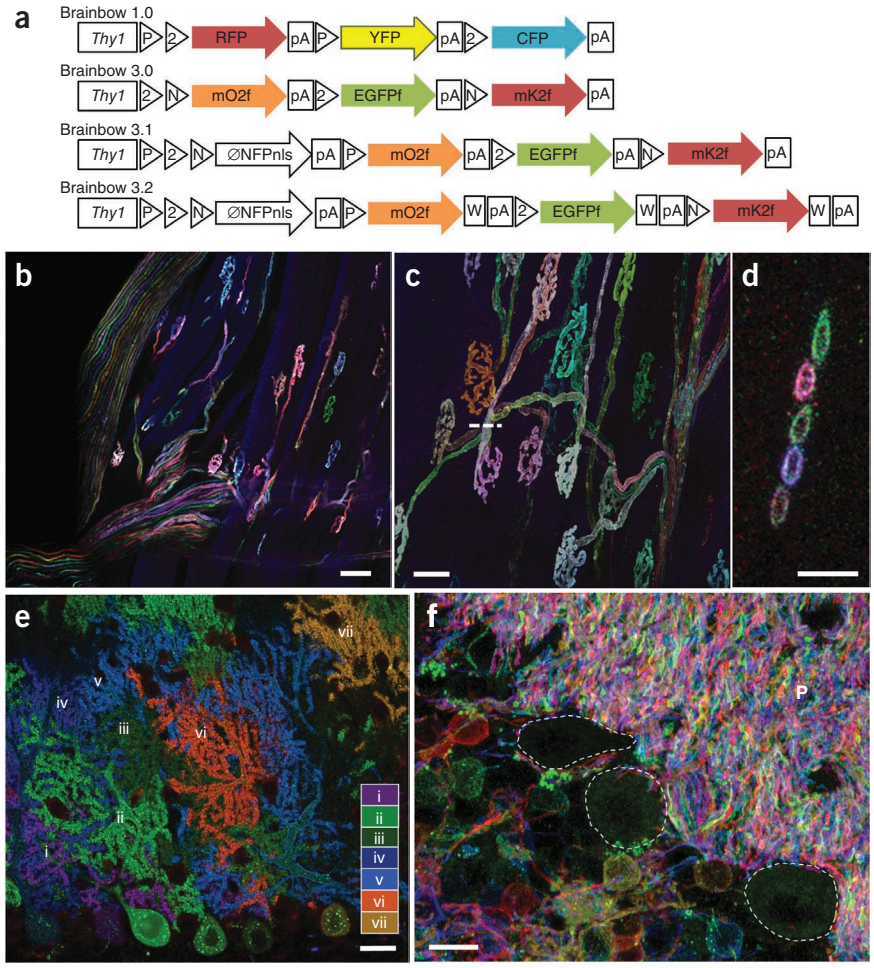

Figure 1 | Brainbow 3 transgenic mice. (**a**) Brainbow constructs and transgenic mice. Brainbow 1.0 is described in ref. 15. Brainbow 3.0 incorporates farnesylated ('f'), antigenically distinct XFPs: mOrange2f (mO2f), EGFPf and mKate2f (mK2f). Brainbow 3.1 incorporates a nuclear-targeted nonfluorescent XFP (ØNFPnls) in the first (default) position. Brainbow 3.2 incorporates a woodchuck hepatitis virus post-transcriptional regulatory element (W) into Brainbow 3.1. P, *loxP* site; 2, *lox2272*; N, *loxN*; pA, polyadenylation sequence. (**b**,**c**) Low- (**b**) and high-power (**c**) views of muscles from a Brainbow 3.0 (line D) Islet-Cre mouse, showing terminal axons and neuromuscular junctions in extraocular muscle. (**d**) Rotated image along dashed bar in **c** showing five motor axons labeled in distinct colors. The open circles show that farnesylated XFPs mark plasma membranes more than cytoplasm. (**e**) Cerebellum from a Brainbow 3.1 (line 3) L7-Cre mouse. The ten Purkinje cells in this field are labeled by at least seven distinct colors (antibody amplified and numbered i–vii). Because Cre is selectively expressed by Purkinje cells in the L7-Cre line, no other cell types are labeled. (**f**) Cerebellum from a Brainbow 3.2 (line 7) CAGGS-CreER mouse showing granule native fluorescence in red, pink, yellow, green, cyan, blue and brown. P, parallel fibers in molecular layer. Purkinje cell bodies, which are unlabeled, are outlined. Scale bars: 50 µm (**b**), 20 µm (**c**,**e**), 5 µm (**d**), 10 µm (**f**).

incompatible wild-type and mutant *loxP* sites are concatenated so that Cre recombinase yields a stochastic choice among XFPs (**Fig. 1a**). We also retained two other features of the Brainbow 1 strategy. First, we used neuron-specific regulatory elements from the *Thy1* gene[14] because it promotes high levels of transgene expression in many, although not all, neuronal types; other promoter-enhancer sequences that we tested support considerably lower levels of expression[21]. Second, we generated transgenic lines by injection into oocytes because this method leads to integration of multiple copies of the cassette and, thus, a broad spectrum of outcomes[15,28]; by contrast, knock-in lines generated by homologous recombination contain one or two copies of the cassette (as heterozygotes or homozygotes, respectively) and, consequently, a smaller number of possible color combinations[17–20].

Design of Brainbow 3.1 and 3.2 transgenes

In Brainbow 1, 2 and 3.0 (**Fig. 1a**) and ref. 15, one XFP is expressed 'by default' in Cre-negative cells. The presence of a default XFP has both drawbacks and advantages. In cases of limited Cre expression, this XFP is expressed in a majority of cells, reducing spectral diversity among recombined neurons. On the other hand, incorporation of a default XFP allows one to screen numerous lines in the absence of a Cre reporter to assess the number and types of cells in which XFPs could be expressed following recombination.

To eliminate the default XFP while retaining the ability to assess expression in the absence of Cre, we adopted the following strategy. First, we incorporated three rather than two pairs of incompatible *loxP* sites, which allowed insertion of a 'stop' cassette[29] into a first position. With this modification, the three XFPs were expressed only in Cre-positive neurons, giving more spectral diversity. Second, we inserted a fourth XFP, Phi-YFP (from the hydrozoon *Phialidium*)[4], which is antigenically distinct from the other three, into the stop cassette. We mutated Phi-YFP to eliminate its endogenous fluorescence (PhiYFP Y65A), fused it to a nuclear localization sequence and generated antibodies against it in rat. In Brainbow 3.1 mice generated from this cassette (**Fig. 1a**), one can screen sections with rat anti–Phi-YFP before Cre recombination (**Supplementary Fig. 1**).

Finally, we inserted a sequence that stabilizes mRNAs, called a woodchuck hepatitis virus post-transcriptional regulatory element (WPRE), into the 3′ untranslated sequences following each XFP. The WPRE has been used in many cases to increase protein levels produced by viral vectors and transgenes[30,31]. We call lines incorporating the WPRE 'Brainbow 3.2' (**Fig. 1a**).

Characterization of Brainbow 3 mice

We generated 31 lines of transgenic mice from the Brainbow 3.0, 3.1 and 3.2 cassettes. Offspring were crossed with several Cre transgenic lines[32–37], leading to multicolor spectral labeling of neuronal populations in numerous regions including cerebral cortex, brainstem, cerebellum, spinal cord and retina (**Fig. 1b–f**, **Supplementary Table 2**, **Supplementary Fig. 2** and **Supplementary Videos 1** and **2**). The intensity of expression varied markedly among lines, making quantitative comparison of dubious value, but the most

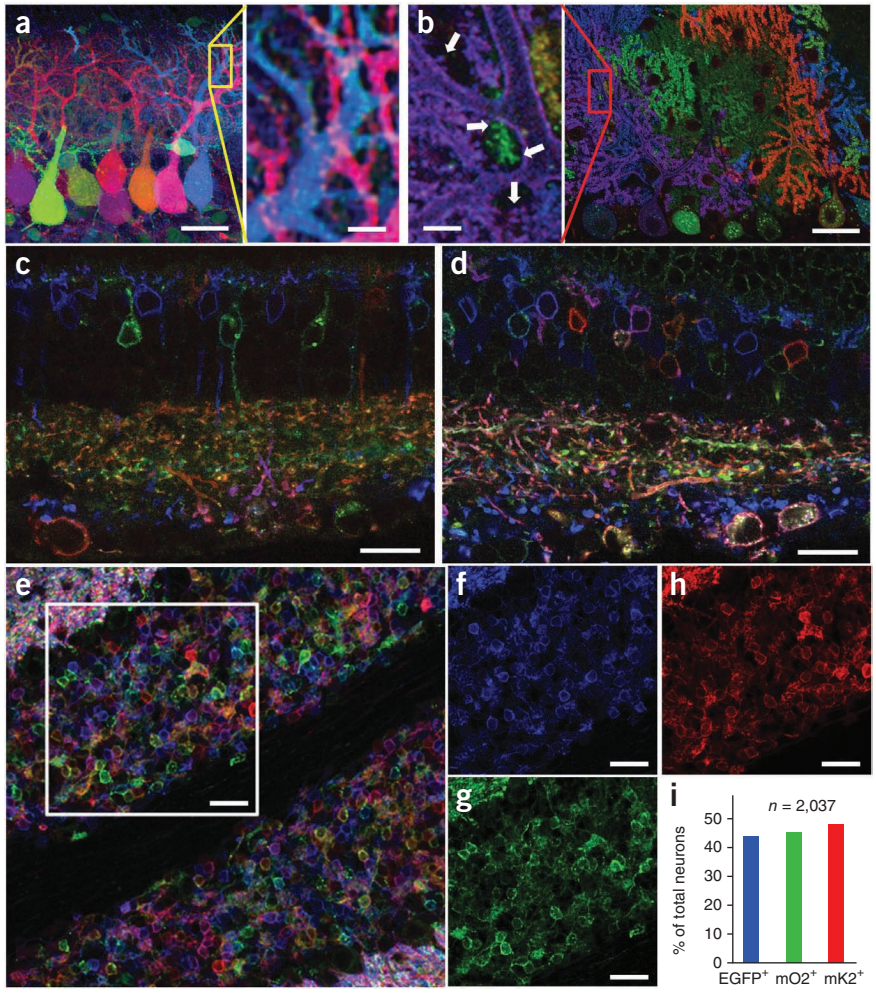

Figure 2 | Improved visualization of neurons in Brainbow 3 mice. (**a**,**b**) Cerebellum from Brainbow 1.0 (**a**) and Brainbow 3.1 (line 3) L7-Cre (**b**) mice. Insets show high-magnification views of boxed regions. The farnesylated XFPs clearly label the fine processes and dendritic spines (**b**, inset arrows), which are missing in the cytoplasmic labeling (**a**, inset). (**c**,**d**) Retina from a Brainbow 3.0 (line D) Islet-Cre mouse expressing EGFP (blue), mOrange2 (green) and mKate2 (red). Intrinsic XFP fluorescence (**c**) and a nearby section immunostained with chicken anti-GFP, rabbit anti-mOrange2 and guinea pig anti-mKate2 (**d**) are shown. (**e**–**h**) Immunostained cerebellum section from Brainbow 3.2 (line 7) parvalbumin-Cre mouse. Separate channels of region boxed in **e** are shown in **f**–**h**. (**i**) Fraction of all labeled neurons that express EGFP, mOrange2 (mO2) or mKate2 (mK2) (n = 2,037 neurons from 15 regions of two brains). Scale bars: 40 µm (**a**,**b**), 20 µm (**c**,**d**), 25 µm (**e**–**g**), 10 µm (insets).

strongly expressing lines were those that incorporated the WPRE (Brainbow 3.2).

Analysis of these lines confirmed their advantages over Brainbow 1 and 2 lines[15]. First, the use of farnesylated XFPs led the XFPs to concentrate at the plasma membrane (**Fig. 1d**). As a consequence, somata were less intensely labeled in Brainbow 3 than in Brainbow 1 mice, so processes could be visualized without saturation of the somata (**Fig. 2a**,**b** and **Supplementary Fig. 3**). Use of farnesylated XFPs also improved labeling of fine processes and dendritic spines (**Fig. 2a**,**b**). Second, the ability to immunostain all three XFPs led to enhancement of the intrinsic fluorescence without loss of color diversity (**Fig. 2c**,**d** and **Supplementary Fig. 4**). Third, XFP fluorescence was visible only in Cre-positive cells, thereby correcting the color imbalance caused by default XFP expression in cells that were Cre negative or cells that expressed Cre at low levels in Brainbow 1 and 2 lines (**Fig. 2e**–**i** and **Supplementary Fig. 5**). Thus, Brainbow 3 lines are likely to be more useful than Brainbow 1 and 2 lines for multicolor labeling.

Brainbow with self-excising Cre recombinase

In Brainbow 1–3 lines, the cassette encodes XFPs separated by *loxP* sites; Cre recombinase is supplied from a separate transgene. For analysis of connectivity in mouse mutants, breeding mice with two transgenes (Brainbow and *Cre*) into an already complex background is cumbersome. We therefore attempted to combine constructs encoding XFPs and Cre in a single cassette. In this transgene, called 'Autobow', we substituted a self-excising Cre recombinase[38] for the stop sequences in Brainbow 3.1 (**Fig. 3a**). The *Thy1* regulatory elements lead to expression of Cre in differentiated neurons; Cre then simultaneously activates an XFP and excises itself.

We generated three founder mice using this construct. Two were analyzed as adults, and both of these exhibited combinatorial expression of XFPs in multiple neurons (**Fig. 3b** and **Supplementary Fig. 2e**). We were concerned that precocious Cre activation in the germ line might lead to loss of the cassette. We therefore established a line from the third founder and examined mice in the second and sixth generations. Color range was limited in this line, perhaps because only a few copies had been integrated into the genome, but the variety of colors and level of expression were similar in both generations (**Fig. 3c**,**d**). Thus, Autobow transgenes can be stably maintained.

Brainbow using Flp recombinase and *FRT* sites

A second recombination system, orthogonal to Cre-*loxP*, could be used to independently control expression of distinct XFPs in, for example, excitatory and inhibitory neurons. In this way, the color of a neuron could denote cell identity, a feature lacking in currently available Brainbow lines[15,17–20]. We therefore tested a second recombination system, in which Flp recombinase acts on Flp recombinase target (*FRT*) sites. The Flp-*FRT* system has been used in conjunction with Cre-*loxP* in mice[16] and in Brainbow-like transgenes in *Drosophila*[24,25].

We tested previously described mutant *FRT* sites[39,40] to find incompatible sets (**Supplementary Fig. 6**) and used these sets to construct 'Flpbow' lines (**Fig. 4a**). In one cassette, we fused the XFPs to an epitope tag[41], which allowed for discrimination of cells labeled by Cre- and Flp-driven cassettes (**Supplementary Fig. 7**).

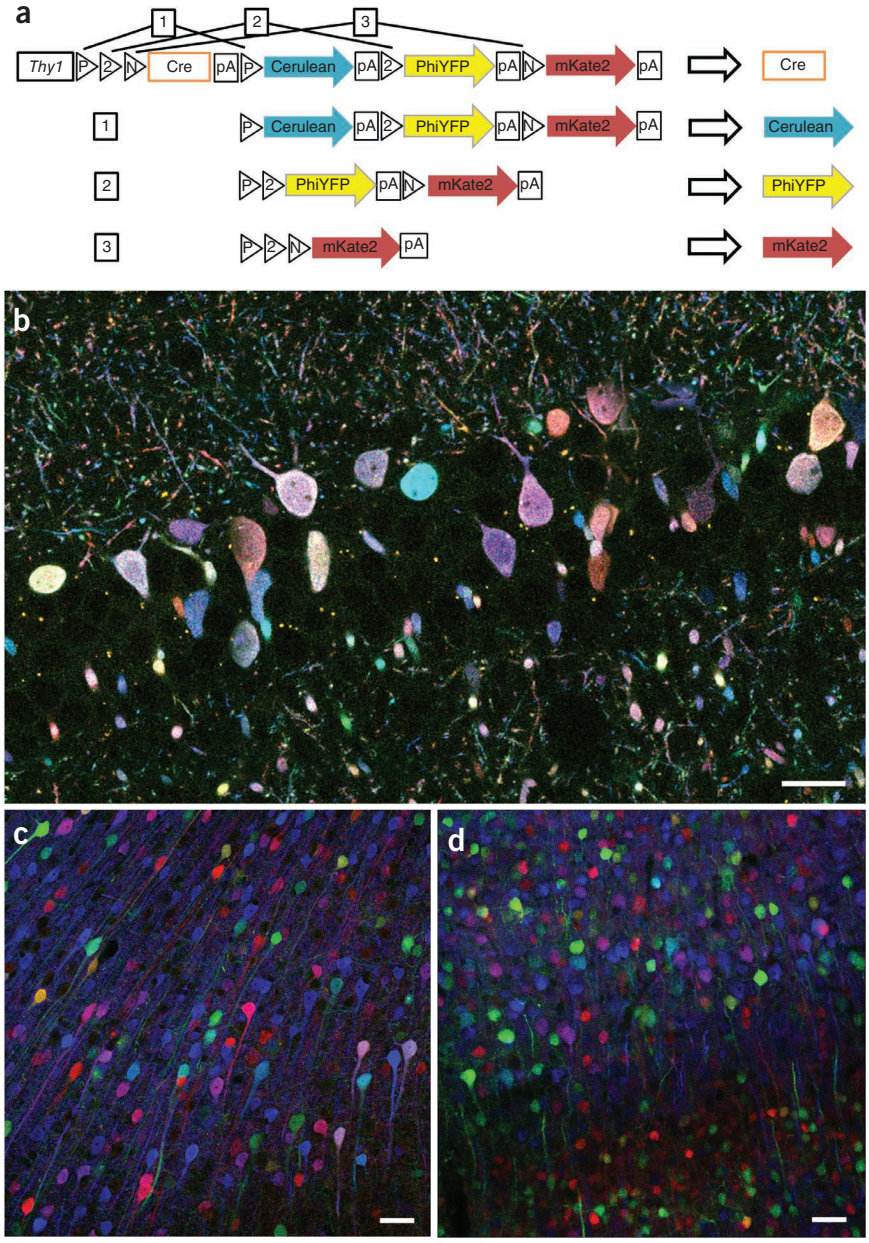

Figure 3 | Autobow. (**a**) Schematic of the Autobow construct and the steps that lead to expression of the three XFP combinations (outcomes 1–3). P, *loxP* site; 2, *lox2272*; N, *loxN*; pA, polyadenylation sequence. (**b**) Labeling of hippocampal neurons by Autobow in founder 3. The 20 large neurons (diameter <5 µm) in this section are labeled in 20 distinct colors. Antibody-amplified Cerulean, PhiYFP and mKate2 are in blue, green and red, respectively. (**c**,**d**) Cortical neurons of an Autobow mouse line in the second (**c**) and sixth (**d**) generations. Antibody-amplified Cerulean, PhiYFP and mKate2 are as in **b**. Scale bars, 50 µm.

When Flpbow mice were mated to Flp-expressing mice[42,43], we observed multicolor labeling (**Fig. 4b**,**c**). Although the few lines tested to date exhibit narrow expression patterns, these results demonstrate that Flp- and Cre-based Brainbow systems can be used in combination.

Brainbow adeno-associated viral vectors

In parallel to developing Brainbow transgenic lines, we generated adeno-associated viral (AAV) vectors to provide spatial and temporal control over expression and to make the method applicable to other species. Because the Brainbow 3.1 cassette described above is >6 kilobase pairs (kb), but the capacity of AAV vectors is <5 kb, we re-engineered the cassette. On the basis of results from initial tests (**Supplementary Fig. 8**), we devised a scheme in which *loxP* sites with left or right element mutations[44] were used for unidirectional Cre-dependent inversion (**Fig. 5a**,**b**). Farnesylated XFPs were positioned in reverse orientation to prevent Cre-independent expression, and WPRE elements were added to increase expression. In this design, recombination can lead to three outcomes from two XFPs: XFP1, XFP2 or neither. We generated two AAVs with two XFPs each, such that co-infection would lead to a minimum of eight hues ($3 \times 3 - 1$; **Fig. 5c**). Because AAV can infect cells at high multiplicity, the number of possible colors is $\gg 8$. An additional feature is that excision of the non-expressed XFP in a second step (**Fig. 5a**) enhances and equalizes expression of the remaining XFP (**Fig. 5d**,**e**).

We infected cortex, cerebellum and retina of Cre transgenic mice with these vectors. When examined 3–5 weeks later, neurons were labeled in multiple colors (**Fig. 5f–j** and **Supplementary Video 3**). Near injection sites, high levels of infectivity led to coexpression of all XFPs in single cells so that neurons appeared gray or white. The variety of colors increased with distance from these sites and then decreased again in sparsely injected regions, presumably because each labeled neuron received only one virion (**Supplementary Fig. 9**).

Methods to optimize Brainbow imaging

Obtaining high-quality images from of tissues expressing Brainbow transgenes is challenging. Because colors are derived by mixing images of multiple fluorophores over a wide range of concentrations, factors that differentially affect the labels degrade the final image. In addition, it is usually necessary to image a tissue volume rather than a single section, so methods for taking image stacks must be optimized. Here we summarize guidelines for imaging Brainbow tissue.

Sample preparation. To minimize background, section thickness should be less than the working distance of the objective, generally <100 µm for high–numerical aperture (high NA) lenses. It is also important to match the refractive indices of the immersion medium and the sample because chromatic aberrations caused by mismatches between these values lead to spatial offsets between color channels (**Supplementary Fig. 10**). Commercial antifade

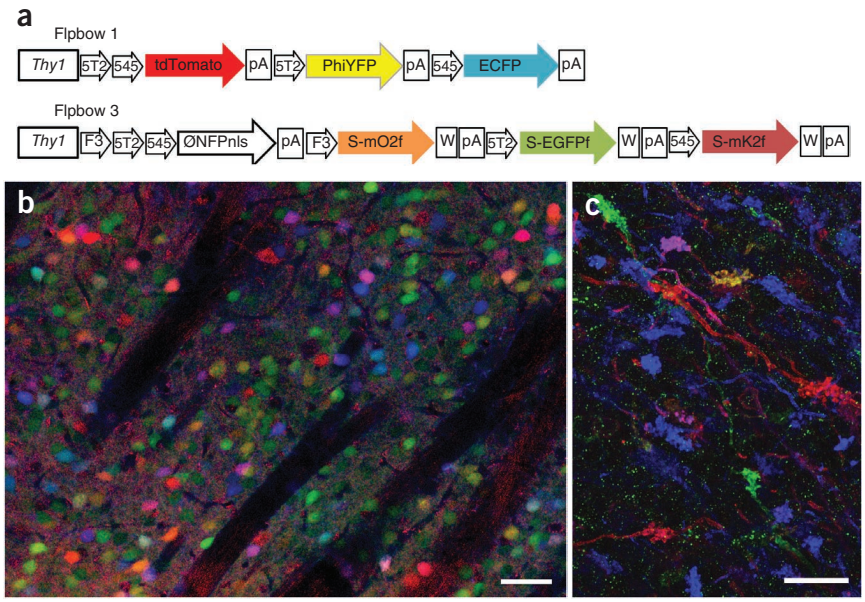

Figure 4 | Flpbow. (**a**) Schematics of Flpbow transgenes. In Flpbow 1, the *loxP* sites of Brainbow 1.0 were replaced by the incompatible *FRT* sites Frt5T2 and Frt545. In Flpbow 3, the *loxP* sites of Brainbow 3.2 were replaced by incompatible *FRT* sites F3, Frt5T2 and Frt545. XFPs were fused to SUMO-Star ('S-'). f indicates farnesylation; pA, polyadenylation sequence; W, woodchuck hepatitis virus post-transcriptional regulatory element. (**b**) Neurons in caudate putamen of a Flpbow 1 Wnt-Flp double transgenic. Neurons are labeled by at least nine colors (red, orange, yellow, yellow-green, green, cyan, blue, purple and pink). Native fluorescence of ECFP, tdTomato and antibody-amplified PhiYFP are in blue, red and green, respectively. (**c**) Mossy fibers in a Flpbow3 Wnt-Flp double transgenic. Fluorescence of antibody-amplified EGFP, mOrange2 and mKate2 are in blue, red and green, respectively. Scale bars: 50 µm (**b**), 20 µm (**c**).

mountants such as Vectashield (Vector Labs) or ProLong Gold (Invitrogen) that have refractive indices of ~1.47 are optimal for objectives that use glycerin as the immersion medium. Polyvinyl alcohol mountants (such as Mowiol 4-88; Sigma-Aldrich) provide a better match for oil-immersion (refractive index of ~1.52) objectives.

Confocal laser scanning microscopy. Epifluorescence microscopy can be used for imaging thin sections (<10 µm) or monolayer cultures, but confocal microscopes are preferable for thick specimens because they decrease contamination by light from outside the plane of focus. Newly developed two-photon multi-XFP imaging techniques are also useful[45–47]. Apochromatic or fluorite microscope objectives that are corrected for three or more colors are strongly recommended. Most lens manufacturers specify preferred oils and coverslips. Using the wrong oil or coverslip degrades the sharpness of focus and increases chromatic aberration.

Fluorophores with overlap in the excitation or emission spectra should be imaged sequentially rather than simultaneously to minimize fluorescence cross-talk and thereby optimize color separation. Laser power should be set as low as possible for several reasons. First, all planes are bleached as each image plane is scanned, so generation of stacks leads to gradual bleaching and decreased signal through the stack. Second, because each fluorophore bleaches at a different rate, colors may shift during imaging. Third, linear signaling requires that fluorophores emit photons at submaximal rates; at higher excitation intensities, only the out-of-focus signal is increased[48]. Fourth, if one fluorophore species is saturated but another is not, small changes in laser power will affect the fluorophore intensities differently, leading to color change. With high-NA objectives, a laser power of just a few milliwatts is saturating; this is generally a small percentage of the total power the laser can provide.

With laser power adjusted to a low level, the photomultiplier-tube voltages and digital gains must be set to relatively high values. In some confocal microscopes it is possible to compensate for signal loss from deep layers through automatic adjustment of laser power, photomultiplier-tube voltage or digital gain as a function of depth. Imaging parameters can be adjusted to obtain images with similar signal ranges throughout the stack.

Image processing. Brainbow images must be postprocessed to maximize color information, but care is needed to avoid introducing artifacts. Often one begins by reducing noise. Because confocal laser scanning of multicolor stacks is generally done at speeds of ~1 µs per pixel or less to save time, the small number of photons collected for each pixel gives rise to sufficient shot noise to cause perceptible local color differences. This problem can be minimized by slower scanning or averaging of multiple scans, but when this is infeasible, simple filtering and deconvolution methods are helpful (**Fig. 6a–c**). For example, median or Gaussian filters with radii of 0.5–2 pixels reduce color noise, but at the expense of resolution. Deconvolution algorithms (Online Methods) are more challenging to use than simple filters but can remove color noise without compromising spatial resolution (**Supplementary Fig. 11**).

Subsequent processing steps can expand the detectable color range and correct for color shifts (**Fig. 6d,e**). To obtain easily perceived color differences, pixel intensity values for each channel in each image are normalized to the same minimum and maximum intensity values for that color in the whole image stack. This linearly stretches all channels and images to the full dynamic range. Color shifts also arise because illumination strength is generally uneven across the imaging field and differs among lasers. This effect can be attenuated by intensity or shading correction for each channel[46,49]. The resulting composite RGB images provide maximum color separation for viewing by eye (**Fig. 6f**).

DISCUSSION

The goal of the work reported here was to design, generate and characterize improved reagents for multicolor Brainbow imaging of neurons in mice. First, we generated new transgenic lines that overcome some limitations of the Brainbow 1 and 2 lines that are currently available[15]. The improvements were the substitution of XFPs (especially red and orange fluorescent proteins)

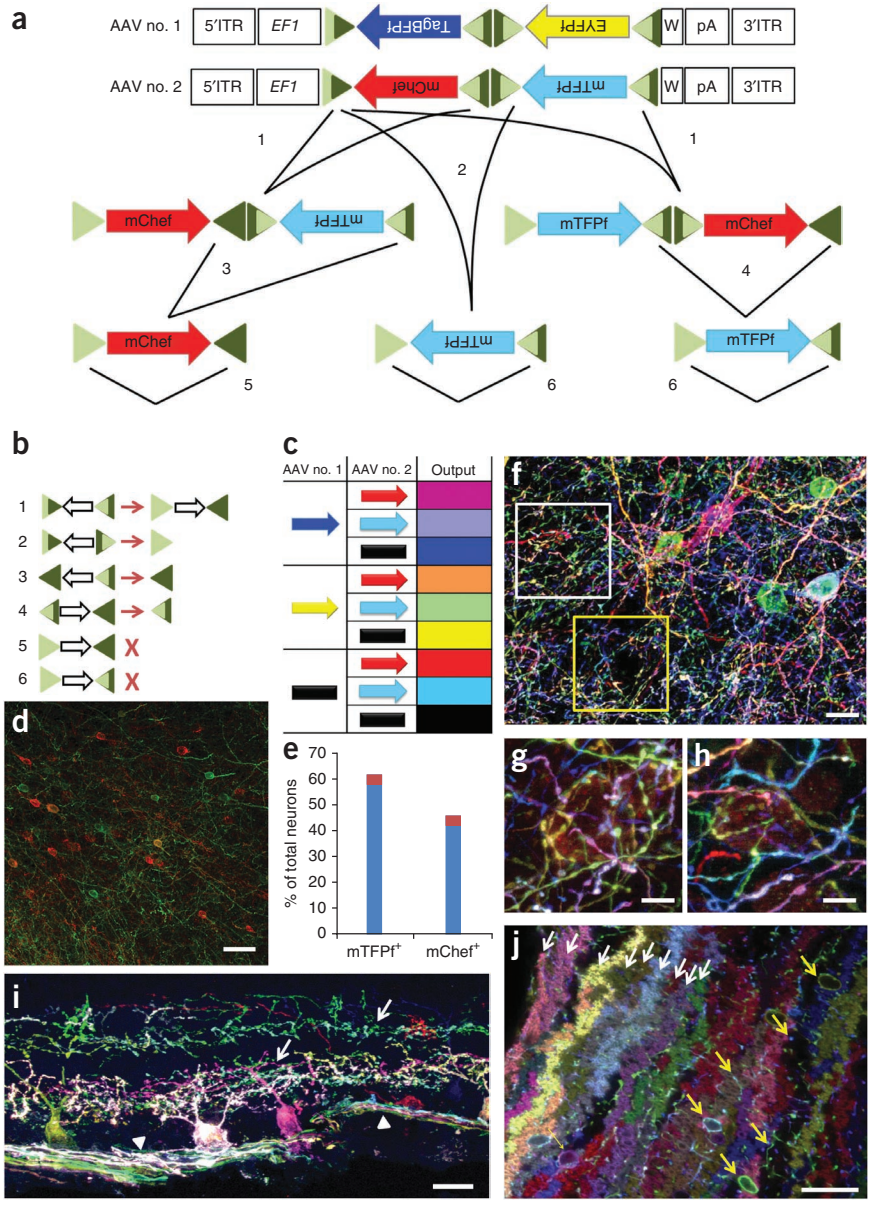

Figure 5 | Brainbow AAV. (**a**) AAV Brainbow constructs and recombination scheme. Farnesylated TagBFP and EYFP or mCherry and mTFP were placed in reverse orientation between mutant *loxP* sites. *EF1α*, regulatory elements from elongation factor 1α gene; W, woodchuck hepatitis virus post-transcriptional regulatory element; pA, polyadenylation sequence; mChef, mCherryf; triangles, *loxP* mutants and their recombination products (dark and light green sectors indicate wild-type and mutant portions of *loxP* sites, respectively); 1–6, recombination events. (**b**) Outcomes of recombination events numbered in **a**. Unfilled arrows, direction of intervening cDNA. An X signifies that a fully mutant (light green) *loxP* site cannot serve as substrate for Cre. (**c**) Eight color outcomes resulting from pairs of Brainbow AAVs following recombination as shown in **a**. This is a minimum value because it does not account for differences in relative intensity of the four XFPs. (**d**,**e**) Test of color balance. The mTFPf-mChef AAV vector was injected at low titer into the cortex of a Thy1-Cre mouse, and neurons of each color were counted. An image from the cortex (**d**) and the fraction of neurons expressing mTFPf (58%) and mChef (42%; n = 1,523 neurons in four sections of three mice; s.d. in red) are shown. (**f**–**h**) Cortex of parvalbumin (PV)-Cre mice injected with the two Brainbow AAVs. High-magnification views of adjacent planes from the yellow (**g**) and white (**h**) boxed regions in **f** are shown. (**i**) Retina from AAV-injected mouse expressing Cre in retinal ganglion cells. Arrows, dendrites; arrowheads, axons. (**j**) Cerebellum from AAV-injected PV-Cre mouse. Fan-shaped dendrites of Purkinje cells (white arrows) and interneurons (yellow arrows) are indicated. In **f**–**j**, antibody-amplified mTFP and EYFP are in green, TagBFP is in blue and mCherry is in red. Scale bars: 100 μm (**d**), 20 μm (**f**), 10 μm (**g**,**h**), 50 μm (**i**,**j**).

that are more photostable and less prone to aggregation than those used initially; use of XFPs with minimal sequence homology so they could be immunostained separately; farnesylation of the XFPs for even staining of somata and the finest processes; insertion of a stop cassette to increase color variety by eliminating broad expression of a default XFP; inclusion of a nonfluorescent marker in the default position to facilitate screening of multiple lines; and insertion of a WPRE to boost expression (**Figs. 1** and **2**). These lines, which incorporate regulatory elements from the *Thy1* gene, enable marking of many but not all neuronal types. To date, elements tested other than those from the *Thy1* gene do not support the high expression levels needed to image Brainbow 1 and 2 material. The ability to immunostain provided by Brainbow 3 cassettes may allow weaker promoters to be used.

Second, we designed two additional transgenes and performed initial tests to demonstrate that they can be used effectively *in vivo*.

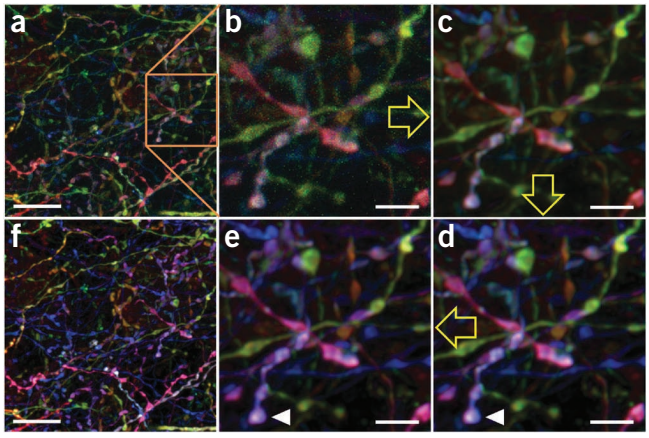

Figure 6 | Processing a Brainbow image. (**a**) Original image from parvalbumin-Cre mouse cortex injected with mixed Brainbow AAVs. (**b**) Region boxed in **a**. (**c**) Deconvolution, to decrease noise without sacrificing spatial resolution. (**d**) Intensity normalization, to expand perceptible color range. (**e**) Color-shift correction (**Supplementary Fig. 10**). (**f**) Fully processed image. Yellow arrows indicate the sequence of image processing. White arrowheads indicate corresponding objects in the original and color shift–corrected images. Scale bars, 10 μm (**a**,**f**), 3 μm (**b**–**e**).

One construct, called Autobow, incorporates a self-excising Cre recombinase. Autobow lacks the temporal and spatial control afforded by the use of specific Cre lines or ligand-activated Cre (CreER). However, because it does not require the generation of double transgenics, it may be useful for rapid screening of neuronal morphology in mutant mice or mice submitted to various experimental interventions (such as drug treatments). The other novel transgene, Flpbow, replaces *loxP* sites with *FRT* sites so that recombination can be controlled by Flp recombinase rather than Cre recombinase. Flpbow 3 also incorporates an epitope tag so that XFPs in Flpbow can be distinguished immunohistochemically from XFPs in Brainbow. By using Cre and Flp transgenic lines with distinct, defined specificities, it should be possible to map separate sets of neurons in a single animal.

Finally, we generated Brainbow AAV vectors. These, along with recently described Brainbow herpes viral vectors[50], may be more useful than Brainbow transgenic mice in some situations. Similar to Autobow, they avoid the need for double-transgenic animals. Because the time of infection can be varied, these vectors provide an alternative to CreER for temporal control. Moreover, localized delivery of AAVs enables the tracing of connections from known sites to multiple targets and discrimination of long-distance inputs from local connections.

The three most broadly useful Brainbow 3 lines (Brainbow 3.0 line D, Brainbow 3.1 line 3, Brainbow 3.1 line 18 and Brainbow 3.2 line 7) have been provided to Jackson Laboratories (http://www.jax.org/; stock numbers 21225–21227) for distribution. The two AAVs shown in **Figure 5** can be obtained from the University of Pennsylvania Vector Core (http://www.med.upenn.edu/gtp/vectorcore/). Plasmids used to generate Brainbow 3.0, 3.1, and 3.2, Autobow and Flpbow 1.1 and 3.1 mice are available through Addgene (http://www.addgene.org/).

METHODS

Methods and any associated references are available in the online version of the paper.

Accession codes. Addgene plasmids: 45176, 45177 (Brainbow 3.0), 45178 (Brainbow 3.1), 45179 (Brainbow 3.2), 45182, 45187 (Autobow), 45180 (Flpbow 1.1), 45181 (Flpbow 3.1).

Note: Supplementary information is available in the online version of the paper.

ACKNOWLEDGMENTS

This work was supported by grants from the US National Institutes of Health (5U24NS063931) and the Gatsby Charitable Foundation and by Collaborative Innovation Award no. 43667 from the Howard Hughes Medical Institute. We thank S. Haddad for assistance with mouse colony maintenance; X. Duan, L. Bogart and J. Lefebvre for testing Brainbow mice and AAVs; R.W. Draft for valuable discussions and advice; R.Y. Tsien (University of California, San Diego) for mOrange2 and TagRFPt; and D.M. Chudakov (Institute of Bioorganic Chemistry of the Russian Academy of Sciences) for TagBFP, PhiYFP, mKate2 and eqFP650.

AUTHOR CONTRIBUTIONS

D.C., K.B.C. and T.L. performed experiments. D.C., J.W.L. and J.R.S. designed experiments, interpreted results and wrote the manuscript.

COMPETING FINANCIAL INTERESTS

The authors declare no competing financial interests.

1. Tsien, R.Y. The green fluorescent protein. *Annu. Rev. Biochem.* **67**, 509–544 (1998).
2. Heim, R. & Tsien, R.Y. Engineering green fluorescent protein for improved brightness, longer wavelengths and fluorescence resonance energy transfer. *Curr. Biol.* **6**, 178–182 (1996).
3. Rizzo, M.A., Springer, G.H., Granada, B. & Piston, D.W. An improved cyan fluorescent protein variant useful for FRET. *Nat. Biotechnol.* **22**, 445–449 (2004).
4. Shagin, D.A. *et al.* GFP-like proteins as ubiquitous metazoan superfamily: evolution of functional features and structural complexity. *Mol. Biol. Evol.* **21**, 841–850 (2004).
5. Ai, H.W., Henderson, J.N., Remington, S.J. & Campbell, R.E. Directed evolution of a monomeric, bright and photostable version of *Clavularia* cyan fluorescent protein: structural characterization and applications in fluorescence imaging. *Biochem. J.* **400**, 531–540 (2006).
6. Subach, O.M. *et al.* Conversion of red fluorescent protein into a bright blue probe. *Chem. Biol.* **15**, 1116–1124 (2008).
7. Ai, H.W., Shaner, N.C., Cheng, Z., Tsien, R.Y. & Campbell, R.E. Exploration of new chromophore structures leads to the identification of improved blue fluorescent proteins. *Biochemistry* **46**, 5904–5910 (2007).
8. Karasawa, S., Araki, T., Nagai, T., Mizuno, H. & Miyawaki, A. Cyan-emitting and orange-emitting fluorescent proteins as a donor/acceptor pair for fluorescence resonance energy transfer. *Biochem. J.* **381**, 307–312 (2004).
9. Shaner, N.C. *et al.* Improving the photostability of bright monomeric orange and red fluorescent proteins. *Nat. Methods* **5**, 545–551 (2008).
10. Shaner, N.C. *et al.* Improved monomeric red, orange and yellow fluorescent proteins derived from *Discosoma* sp. red fluorescent protein. *Nat. Biotechnol.* **22**, 1567–1572 (2004).
11. Shcherbo, D. *et al.* Far-red fluorescent tags for protein imaging in living tissues. *Biochem. J.* **418**, 567–574 (2009).
12. Shcherbo, D. *et al.* Near-infrared fluorescent proteins. *Nat. Methods* **7**, 827–829 (2010).
13. Shaner, N.C., Steinbach, P.A. & Tsien, R.Y. A guide to choosing fluorescent proteins. *Nat. Methods* **2**, 905–909 (2005).
14. Feng, G. *et al.* Imaging neuronal subsets in transgenic mice expressing multiple spectral variants of GFP. *Neuron* **28**, 41–51 (2000).
15. Livet, J. *et al.* Transgenic strategies for combinatorial expression of fluorescent proteins in the nervous system. *Nature* **450**, 56–62 (2007).
16. Branda, C.S. & Dymecki, S.M. Talking about a revolution: the impact of site-specific recombinases on genetic analyses in mice. *Dev. Cell* **6**, 7–28 (2004).
17. Snippert, H.J. *et al.* Intestinal crypt homeostasis results from neutral competition between symmetrically dividing Lgr5 stem cells. *Cell* **143**, 134–144 (2010).
18. Red-Horse, K., Ueno, H., Weissman, I.L. & Krasnow, M.A. Coronary arteries form by developmental reprogramming of venous cells. *Nature* **464**, 549–553 (2010).
19. Rinkevich, Y., Lindau, P., Ueno, H., Longaker, M.T. & Weissman, I.L. Germ-layer and lineage-restricted stem/progenitors regenerate the mouse digit tip. *Nature* **476**, 409–413 (2011).
20. Schepers, A.G. *et al.* Lineage tracing reveals Lgr5^{+} stem cell activity in mouse intestinal adenomas. *Science* **337**, 730–735 (2012).
21. Tabansky, I. *et al.* Developmental bias in cleavage-stage mouse blastomeres. *Curr. Biol.* **23**, 21–31 (2013).
22. Gupta, V. & Poss, K.D. Clonally dominant cardiomyocytes direct heart morphogenesis. *Nature* **484**, 479–484 (2012).
23. Pan, Y.A., Livet, J., Sanes, J.R., Lichtman, J.W. & Schier, A.F. Multicolor Brainbow imaging in zebrafish. *Cold Spring Harb. Protoc.* **2011**, pdb.prot5546 (2011).
24. Hampel, S. *et al. Drosophila* Brainbow: a recombinase-based fluorescence labeling technique to subdivide neural expression patterns. *Nat. Methods* **8**, 253–259 (2011).
25. Hadjieconomou, D. *et al.* Flybow: genetic multicolor cell labeling for neural circuit analysis in *Drosophila melanogaster*. *Nat. Methods* **8**, 260–266 (2011).
26. Lang, C., Guo, X., Kerschensteiner, M. & Bareyre, F.M. Single collateral reconstructions reveal distinct phases of corticospinal remodeling after spinal cord injury. *PLoS ONE* **7**, e30461 (2012).
27. Badaloni, A. *et al.* Transgenic mice expressing a dual, CRE-inducible reporter for the analysis of axon guidance and synaptogenesis. *Genesis* **45**, 405–412 (2007).
28. Lichtman, J.W., Livet, J. & Sanes, J.R. A technicolour approach to the connectome. *Nat. Rev. Neurosci.* **9**, 417–422 (2008).

29. Lakso, M. *et al.* Targeted oncogene activation by site-specific recombination in transgenic mice. *Proc. Natl. Acad. Sci. USA* **89**, 6232–6236 (1992).
30. Paterna, J.C., Moccetti, T., Mura, A., Feldon, J. & Büeler, H. Influence of promoter and WHV post-transcriptional regulatory element on AAV-mediated transgene expression in the rat brain. *Gene Ther.* **7**, 1304–1311 (2000).
31. Madisen, L. *et al.* A robust and high-throughput Cre reporting and characterization system for the whole mouse brain. *Nat. Neurosci.* **13**, 133–140 (2010).
32. Hippenmeyer, S. *et al.* A developmental switch in the response of DRG neurons to ETS transcription factor signaling. *PLoS Biol.* **3**, e159 (2005).
33. Srinivas, S. *et al.* Cre reporter strains produced by targeted insertion of *EYFP* and *ECFP* into the *ROSA26* locus. *BMC Dev. Biol.* **1**, 4 (2001).
34. Guo, C., Yang, W. & Lobe, C.G. A Cre recombinase transgene with mosaic, widespread tamoxifen-inducible action. *Genesis* **32**, 8–18 (2002).
35. Zhang, X.M. *et al.* Highly restricted expression of Cre recombinase in cerebellar Purkinje cells. *Genesis* **40**, 45–51 (2004).
36. Rossi, J. *et al.* Melanocortin-4 receptors expressed by cholinergic neurons regulate energy balance and glucose homeostasis. *Cell Metab.* **13**, 195–204 (2011).
37. Campsall, K.D., Mazerolle, C.J., De Repentingy, Y., Kothary, R. & Wallace, V.A. Characterization of transgene expression and Cre recombinase activity in a panel of *Thy-1* promoter-*Cre* transgenic mice. *Dev. Dyn.* **224**, 135–143 (2002).
38. Bunting, M., Bernstein, K.E., Greer, J.M., Capecchi, M.R. & Thomas, K.R. Targeting genes for self-excision in the germ line. *Genes Dev.* **13**, 1524–1528 (1999).
39. McLeod, M., Craft, S. & Broach, J.R. Identification of the crossover site during FLP-mediated recombination in the *Saccharomyces cerevisiae* plasmid 2 μm circle. *Mol. Cell Biol.* **6**, 3357–3367 (1986).
40. Schlake, T. & Bode, J. Use of mutated FLP recognition target (FRT) sites for the exchange of expression cassettes at defined chromosomal loci. *Biochemistry* **33**, 12746–12751 (1994).
41. Peroutka, R.J., Elshourbagy, N., Piech, T. & Butt, T.R. Enhanced protein expression in mammalian cells using engineered SUMO fusions: secreted phospholipase A2. *Protein Sci.* **17**, 1586–1595 (2008).
42. Farley, F.W., Soriano, P., Steffen, L.S. & Dymecki, S.M. Widespread recombinase expression using FLPeR (flipper) mice. *Genesis* **28**, 106–110 (2000).
43. Awatramani, R., Soriano, P., Rodriguez, C., Mai, J.J. & Dymecki, S.M. Cryptic boundaries in roof plate and choroid plexus identified by intersectional gene activation. *Nat. Genet.* **35**, 70–75 (2003).
44. Araki, K., Okada, Y., Araki, M. & Yamamura, K. Comparative analysis of right element mutant *loxP* sites on recombination efficiency in embryonic stem cells. *BMC Biotechnol.* **10**, 29 (2010).
45. Entenberg, D. *et al.* Setup and use of a two-laser multiphoton microscope for multichannel intravital fluorescence imaging. *Nat. Protoc.* **6**, 1500–1520 (2011).
46. Mahou, P. *et al.* Multicolor two-photon tissue imaging by wavelength mixing. *Nat. Methods* **9**, 815–818 (2012).
47. Wang, K. *et al.* Three-color femtosecond source for simultaneous excitation of three fluorescent proteins in two-photon fluorescence microscopy. *Biomed. Opt. Express* **3**, 1972–1977 (2012).
48. Conchello, J.A. & Lichtman, J.W. Optical sectioning microscopy. *Nat. Methods* **2**, 920–931 (2005).
49. Ducros, M. *et al.* Efficient large core fiber-based detection for multi-channel two-photon fluorescence microscopy and spectral unmixing. *J. Neurosci. Methods* **198**, 172–180 (2011).
50. Card, J.P. *et al.* A dual infection pseudorabies virus conditional reporter approach to identify projections to collateralized neurons in complex neural circuits. *PLoS ONE* **6**, e21141 (2011).

ONLINE METHODS

Brainbow constructs. cDNA encoding the following fluorescent proteins were used: EGFP[1], EYFP[2], ECFP[2], mCerulean[3], PhiYFP[4] (Evrogen), mTFP[5] (Allele Biotechnology), TagBFP[6] (Evrogen), EBFP2 (ref. 7) (Addgene), Kusabira-Orange[8], TagRFPt[9], mOrange2 (ref. 9), tdTomato[10], mCherry[10], mKate2 (ref. 11) (Evrogen) and eqFP650 (ref. 12) (Evrogen). A HRAS farnesylation sequence[51] was used to tether XFPs to the cell membrane. A nuclear localization signal (NLS, APKKKRKV) was added to the N-terminal end of PhiYFP(Y65A). WPRE sequence was used to stabilize mRNA and enhance nuclear mRNA export[30,31]. Polyadenylation signals were from the SV40 T antigen for mouse transgenes and from the human growth hormone gene for AAV. Brainbow constructs were assembled by standard cloning methods. A cloning scaffold containing concatenated *loxP* mutant sequences and unique restriction digestion sites was synthesized (DNA2.0, Inc.) to facilitate cloning.

Brainbow modules were cloned into the pCMV- N1 mammalian expression vector (Clontech) for transient mammalian cell expression. Brainbow mouse constructs were cloned into a unique XhoI site in a genomic fragment of *Thy1.2* containing neuron-specific regulatory elements[14]. Brainbow AAV constructs were cloned into vectors provided by the University of Pennsylvania Virus Core. Constructs were tested by expression in HEK293 cells (ATCC) before generation of mice or AAV.

Mice. Transgenic mice were generated by pronuclear injection at the Harvard Genome Modification Core. Mice were maintained on C57B6 or CD-1 backgrounds. Brainbow mice were crossed to mice that expressed Cre or Flp recombinases, including PV-Cre[32], Islet-Cre[33], CAGGS-CreER[34], L7-Cre[35], ChAT-Cre[36], Thy1-Cre[37], Wnt-Flp[43] and Actin-Flp[42]. Both male and female mice were used. All experiments conformed to NIH guidelines and were carried out in accordance with protocols approved by the Harvard University Standing Committee on the Use of Animals in Research and Teaching.

AAV injection. Two Brainbow AAVs were mixed to equal titer (7.5×10^{12} genome copies per ml) before injection. For retina injection, adult mice were anesthetized with ketamine-xylazine by intraperitoneal injection. A small hole was made in the temporal eye by puncturing the sclera below the cornea with a 30 1/2–G needle. With a Hamilton syringe with a 33-G blunt-ended needle, 0.5–1 µl of AAV virus was injected intravitreally. After injections, animals were treated with Antisedan (Zoetis) and monitored for full recovery. For cortex injection, adult mice were anesthetized with isoflurane via continuous delivery through a nose cone and fixed to a stereotaxic apparatus. Surgery took place under sterile conditions with the animal lying on a heating pad. One microliter of 1:5 saline-diluted AAV mix (1.5×10^{12} genome copies per ml) was injected over 10 min. The head wound was sutured at the end of the experiment. One injection of the nonsteroidal anti-inflammatory agent meloxicam was given at the end of the surgery, and mice were kept on a heating pad with accessible moistened food pellets and/or HydroGel until they had fully recovered. The mice were given another dose of meloxicam 1 d later and examined 4–6 weeks after infection.

Antibodies. Expression vectors were constructed to produce His tag fusions of XFPs in *Escherichia coli*. Proteins were produced in bacteria, purified using His Fusion Protein Purification Kits (Thermo Scientific), concentrated to >3 mg/ml, and used as immunogens to produce rat anti-mTFP, chicken anti-EGFP, rat anti-PhiYFP, rabbit anti-mCherry and guinea pig anti-mKate2. (Covance). Chicken anti-EGFP IgY was purified from chicken egg yolks using Pierce Chicken IgY Purification Kit (Thermo Scientific). Other sera were used without purification. Other antibodies used were: rabbit anti-GFP (ab6556, Abcam), rabbit anti-PhiYFP (AB604, Evrogen), chicken anti-SUMOstar (AB7002, LifeSensors), DyLight 405–conjugated goat anti-rat (Jackson ImmunoResearch) and Alexa fluorescent dye–conjugated goat anti-rat 488, anti-chicken 488 and 594, anti-rabbit 514 and 546, and anti–guinea pig 647 (Life Technologies).

Histology. Mice were anesthetized with sodium pentobarbital before intracardiac perfusion with 2%–4% paraformaldehyde in PBS. Brains were sectioned at 100 µm using a Leica vt1000s vibratome. Muscle and retina were sectioned at 20 µm in a Leica CM1850 cryostat or processed as whole mounts. For immunostaining, tissues were permeabilized by 0.5% Triton X-100 with 0.02% sodium azide in StartingBloc (Thermo Scientific) at room temperature for 2 h and then incubated with combinations of anti-XFPs (see above) for 24–48 h at 4 °C. After extensive washing in PBST (0.01 M PBS with 0.1% Triton X-100), all secondary antibodies (1:500) were added for 12 h at 4 °C. Finally, sections and tissues were mounted in Vectashield mounting medium (Vector Labs) and stored at –20 °C until they were imaged.

Antibody combinations used in figures are as follows. In **Figures 1e–h; 2b**,**d–g;** and **4c** and **Supplementary Figures 2a–d**, **4a** and **5**, primary antibodies are chicken anti-GFP (1:2,000), rabbit anti-mCherry (1:1,000, for mOrange2) and guinea pig anti-mKate2 (1:500). Secondary antibodies are Alexa dye–conjugated goat anti-chicken 488, anti-rabbit 546, and anti–guinea pig 647. In **Figure 3b–d** and **Supplementary Figure 2e**, primary antibodies are chicken anti-GFP (for ECFP), rabbit anti-PhiYFP (1:1,000) and guinea pig anti-mKate2. Secondary antibodies are Alexa dye–conjugated goat anti-chicken 488, anti-rabbit 546 and anti-guinea pig 647. In **Figure 4b**, rabbit anti-PhiYFP and Alexa dye–conjugated goat anti-rabbit 514 were used. In **Figure 5d**, primary antibodies are rat anti-mTFP and rabbit anti-mCherry. Secondary antibodies are Alexa dye–conjugated goat anti-rat 488 and anti-rabbit 546. In **Figure 5f–j** and **Supplementary Figure 9**, primary antibodies are guinea pig anti-mKate2 (for TagBFP), rat anti-mTFP (1:1,000), chicken anti-GFP (for EYFP) and rabbit anti-mCherry. Secondary antibodies are Alexa dye–conjugated goat anti-rat 488, anti-chicken 488, anti-rabbit5 46 and anti-guinea pig 647. In **Supplementary Figure 1**, primary antibodies are rat anti-PhiYFP (1:1,000) and rabbit anti-mCherry (1:1,000, for mOrange2). Secondary antibodies are Alexa dye–conjugated goat anti-rat 488 and anti-rabbit 546. In **Supplementary Figure 7**, primary antibodies are rabbit anti-EGFP (1:1,000, for ECFP) and chicken anti-SUMOstar (1:1,000). Secondary antibodies are Alexa dye–conjugated goat anti-rabbi 514 and anti-chicken 594.

Imaging. Fixed brain and muscle samples were imaged using a Zeiss LSM710 confocal microscope. Best separation of multiple fluorophores was obtained by using a 405-nm photodiode laser for TagBFP and DyLight 405, a 440-nm photodiode laser for mTFP, a 488-nm Argon line for EGFP and Alexa 488, a 514-nm

doi:10.1038/nmeth.2450

Argon line for EYFP and Alexa 514, a 561-nm photodiode for mOrange2 and Alexa 546, a 594-nm photodiode for mCherry, mKate2 and Alexa 594 or a 633-nm photodiode for Alexa 647. Images were obtained with 16× (0.8 NA), and 63× (1.45 NA) oil objectives. Confocal image stacks for all channels were acquired sequentially, and maximally or 3D-view projected using ImageJ (NIH). Intensity levels were uniformly adjusted in ImageJ.

Optimal imaging for Brainbow 3 tissue used a Zeiss LSM710 with fixed dichroic mirror combinations of DM455+514/594 to reduce lag time between the two sequential scans. EGFP and mKate2 were excited by 458-nm and 594-nm lasers simultaneously, and fluorescence was collected at 465–580 nm in channel 1 and 605–780 nm in channel 2, respectively. In a subsequent scan, a 514-nm laser was used to excite mOrange2, and fluorescence was collected at 545–600 nm in channel 2. In the antibody-amplified samples, conjugated Alexa dyes normally produced much stronger fluorescence signal than XFPs. The Zeiss microscope we used was optimized for imaging the Alexa 488/546/647 combination. The fixed dichroic mirror was DM488/561/633. Alexa 488 and Alexa 647 were excited by 488-nm and 633-nm lasers simultaneously, and fluorescence was collected at 495–590 nm in channel 1 and 638–780 nm in channel 2, respectively. In the subsequent scan, a 561-nm laser was used to excite mOrange2, and fluorescence was collected at 566–626 nm in channel 2.

51. Hancock, J.F., Cadwallader, K., Paterson, H. & Marshall, C.J.A. CAAX or a CAAL motif and a second signal are sufficient for plasma membrane targeting of ras proteins. *EMBO J.* **10**, 4033–4039 (1991).